Materials Plus
https://ojs.wiserpub.com/index.php/MP/

Research Article

Printability, Performance and Adaptive Moisture Response: Advanced Hygromorphic materials using synergistic properties of keratin and lignin

Warren Grigsby[1*], Sonya Scott[2], Hosea Watson[2,3], Paul Middlewood[2]

[1]Rotorua 3010, New Zealand
[2]AgResearch Ltd, Lincoln Research Centre, Private Bag 4749, Christchurch 8140, New Zealand
[3]University of Canterbury, Private Bag 4800, Christchurch 8041, New Zealand
E-mail: warren.grigsby@henkel.com

Received: 23 September 2023; **Revised:** 23 May 2024; **Accepted:** 5 June 2024

Abstract: Developing materials that respond and adapt to external stimuli are of increasing interest in additive manufacturing as their potential to react to triggers can be used as a response required of a user. As biopolymers, keratin and lignin exhibit macromolecular behaviours influenced by moisture and these properties have been evaluated as four dimensional (4D) responsive hygromorphic materials. Through three dimensional (3D) paste keratin-lignin hydrogel deposition, the integrity, mechanical properties and 4D moisture sorption responses of these materials was found to be enhanced by additives including carrageenan, guar gum and calcium chloride. As an example, inclusion of carrageenan and calcium led to greater dynamic vapour moisture sorption behaviours compared to guar gum. While carrageenan acted to improve mechanical properties, combination with calcium led to lower mechanical performance and plasticization of hydrogels. In contrast, the cross-linking provided by calcium ions reduced liquid water sorption and was found to extend sample mechanical performance on water immersion. Inclusion of guar gum improved keratin-lignin hydrogel deposition, but provided minimal enhancements of material properties or moisture responses. Overall, study findings suggest selective combinations of carrageenan and calcium can produce 4D moisture responsive keratin-lignin hydrogels where these resulting adaptative swell or softening behaviours may be used in hygromorphic material applications.

***Keywords*:** 3D printing; keratin; lignin; moisture sorption; hygromorphic materials; protein cross-linking; carrageenan; guar gum

1. Introduction

3D printing has revolutionised the manufacturing of customised objects, prototyping and material design [1]. Natural-biopolymers (e.g., proteins) and fibres (e.g., cellulose), as natural, renewable, biodegradable materials, have the ability to undergo property changes due to an external stimuli (e.g., temperature, humidity, stretching) [2]. Such a tendency provides an opportunity to create a 4th dimension (4D) to printed materials or for functional components such as automotive motors and sensors [3, 4]. Such 4D responses can include shape or morphology changes stimulated by heat, light, electricity or a change over time [5–9]. As an example, cellulose can undergo a mechanical response on moisture sorption which has been conveyed as a 4D material change programmed into a cellulose-containing biomimetic materials [10]. Other biomaterials such as proteins and polyphenolic lignins also possess a range of inherent properties including physio-chemical responses to moisture [11–14]. These

DOI: https://doi.org/10.37256/3120243698

biopolymers could be similarly utilised in smart material design, particularly as they are commonly available from many sources [15–17].

Our previous paper discussed the use of keratin, derived from wool, hair and feathers [18], and lignin, an organic polymer derived from trees, as co-polymers for 3D paste printing [19]. While additive manufacturing employing biopolymers has tended to focus on biomass polysaccharides [20], keratin, a protein, has been employed in bio-printing and biomedical applications [21] using keratin self-assembly which can be further tuned through molecular composition or cross-linking into hydrogels [22]. There are many reports of lignin use in additive manufacturing applications, most commonly in combinations with thermoplastics in inks or fused deposition modelling (FDM) where lignin-based filament materials are typically associated with less than 70% lignin content [23]. FDM-based printing is projecting vast applications for lignin-based materials as biobased plastics [24]. In considering 4D material responses, two recent papers examine the use of keratin as a shape memory polymer. Lai et al. extracted keratin from human hair and then demonstrated its self-assembly into dense homogenous and continuous nanofibrous networks [25]. Cera et al. developed a hierarchical keratin structure that demonstrated shape memory under application of moisture stimuli [26]. Although lignin use is not reported in 4D printing, there are many examples of this biopolymer applied in composite printing as a reinforcement with polylactic acid [27–30].

Liquid, or vapour-responsive materials are of high interest owing to the abundant nature of the stimulus and the broad range of possible applications [31]. Examples of hygroscopic responsive materials include hydrogels with hydrophilicity that allows them to expand up to 200% of their original volume [32]. Both keratin and lignin each have their own set of unique physiochemical properties which can change or be adapted in the presence of moisture and plasticisers [33–35]. Our previous study examined the combination of lignin and keratin as a novel 3D printed material for potential 4D applications [19]. This paper builds on these promising findings expanding the breadth of modified keratin-lignin formulations and quantifying their 3D printability and dynamic responses to moisture. Ultimately, a study goal is to produce smart hygomorphic 3D printed keratin-lignin materials with defined environmental responses for 4D applications.

2. Materials and methods

2.1 *Materials*

Keratin powder was obtained *via* an established procedure employing aqueous extraction of sheep wool to give an intermediate filament protein (IFP) powder [36]. A 10% keratin stock solution was prepared by dissolving IFP powder in water while maintaining solution pH at either pH 8.3, 11 or 12 using 1 M sodium hydroxide [19]. The lignin used was Indulin AT (Ingevity, USA) and a 20% lignin stock solution prepared as previously described [19]. Guar gum (Sigma), kappa-carrageenan (Sigma) were used as supplied. Calcium chloride (Sigma) was used as a 1M solution. Acetic acid (Sigma) was diluted to 2M concentration before use.

2.1.1 *Hydrogel formulations*

The procedure for preparing aqueous hydrogel pastes was modified from previous work [19] as follows. The required amount of lignin solution (3 g) was combined with keratin solution (30 g) then stirred before the required amount of either guar gum or carrageenan was added. The hydrogel formulation was then heated to 60 °C for 15 minutes with further mixing. Where stated, the required amount of 1M calcium chloride solution was added while stirring for an additional 5 minutes. Each formulation was conditioned at 4 °C for 24 hours before printing.

2.1.2 *Hydrogel 3D printing*

Formulations were printed using an Anycubic i3 Mega 3D printer that had been in-house modified by replacing the thermoplastic print head with an air driven syringe. The syringe nozzle tip had a diameter 0.9 mm. Digital 3D models were prepared for printing (converted to g-code) using Cura slicing software.

For each print (Table 1), the gel printer was primed for extrusion by ‘skirting’: extrusion-tracing the print bed site perimeter, in duplicate, prior to commencing printing. Extrusion multiplier (0.30) and primary height layer (1.36 mm) settings were used and nozzle tip height was adjusted with the G-code offset: z-axis parameter as appropriate to allow space for extrusion. The printing speed ranged between 300-750 mm/min to generate 3D printed patterns of five single-strand beams. Upon determining optimal printing speed for each formulation, five multi-strand beams (specimen bars) were generated as two layer prints of each keratin-lignin hydrogel formulation.

Generally, hydrogel bars were printed to obtain final dimensions of 50 mm × 12 mm × 5 mm (length × width × height).

After allowing to partially dry (*ca*. 2 hours) the printed bars were removed from the printer and air-dried under ambient laboratory conditions (20 °C and 65% RH, 24 hours). Bars transitioned from flexible materials to materials with varied brittleness of *ca*. 4 mm thickness. Samples were conditioned (20 °C and 65% relative humidity, RH) until required testing.

2.1.3 *Post-treatment of printed bars*

For a selection of 3D printed hydrogel bars, a post-printing acid treatment was undertaken via immersion of these bars in 2M acetic acid. Bars were fully immersed in this acid solution for either 10, 30, 120 or 300 seconds. The bars were then recovered, blotted dry and left to air dry for 3 days in a fume hood before further conditioning as above.

2.2 *3D printed bar testing*

2.2.1 *SEM analysis*

Samples were dried by storing in a desiccant cabinet overnight and mounted on an aluminium tab with conductive carbon tape. The sample images were collected on a Hitachi TM-3030Plus Tabletop SEM using SE standard mode and 15 kV.

2.2.2 *Relative humidity testing*

Equilibrated sample bars (20 °C and 65% RH) were accurately weighed (4 dp balance), then placed in a relative humidity chamber (Surface Measurement Systems, GenRH-A) set at the stated humidity (40 to 90% RH) at 20 °C. Each bar was recovered and weighed at defined time intervals over a total equilibration period of 30 minutes. The percentage weight change (%Wt) of the bars was then calculated using Equation 1. Additionally, a weight change rate (%Wt/min) was calculated from the overall weight loss or gain over the 30 minutes equilibration period using Equation 2.

$$\%\text{Weight change: } \%Wt = \frac{weight_{final} - weight_{initial}}{weight_{initial}} \times 100 \quad (1)$$

$$\text{Rate of \%Weight change: } \%Wt/min = \left(\frac{weight_{final} - weight_{initial}}{weight_{initial}} \times 100\right)/30 \quad (2)$$

2.2.3 *Water immersion testing*

Conditioned sample bars were accurately weighed before their immersion in water (20 °C). Bars were fully submerged during testing and only briefly removed to record weights at defined times. At each measurement time, bars were removed from the water, blotted to remove free water, and then weighed before being immediately returned to the water. As above, the %weight change of the bars and rate of change were calculated according to Equations 1 and 2.

2.2.4 *Three-point bending*

Prior to mechanical testing, printed hydrogel bars were accurately measured using a digital vernier caliper (+/- 0.01 mm) and mounted on an Instron 4202 fitted with a three-point bending fixture (24 mm span). Testing was undertaken at a strain rate 0.01 mm/mm min until specimen failure was achieved. Modulus of elasticity and flexural strength were calculated according to ASTM D790 (02) methodology.

Differential scanning calorimetry*:* Differential scanning calorimetry (DSC) was performed on a TA Instruments (USA) Q1000. Samples (~2-4 mg) cut from conditioned bars were placed in aluminium hermetic pans and crimp sealed. Samples were heated under a nitrogen purge using a heat/cool/heat cycle, initially heating to 200 °C at a temperature ramp rate of 10 °C/min before cooling to -20 °C (5 °C/min) and then heating to 200 °C (10 °C/min).

Dynamic mechanical thermal analysis*:* Dynamic mechanical thermal analysis (DMTA) was conducted in three-point bending mode (40 mm span) using a TA Instruments RSA-G2 instrument fitted with an immersion cup. Conditioned (23˚C, 50% RH) hydrogel bars (10 x 4 mm cross-section) were trimmed to a nominal length. Samples were mounted in the DMTA and analysis commenced. Within 2 minutes the immersion cup filled with

water (23 °C) and testing continued. Samples were evaluated isothermally (23 °C) employing a 1.0 Hz frequency and 0.01% strain until sample failure or excessive swelling was observed.

3. Results

3.1 *Printability of differing hydrogel formulations*

In order to match keratin-lignin (KL) formulation compositions with printability requirements, hydrogel formulations [19] were prepared with either carrageenan (car) or guar gum (gg) thickening additives [37, 38] together with changes in pH of the keratin solution and additions of calcium chloride (Table 1). Favourable printability characteristics were achieved *via* surveying a range of compositions ensuring sufficient formulation viscosity and flow, in combination with shape retention of the hydrogel on drying suitable for material testing evaluations. In brief, hydrogel formulations with either 30% carrageenan or guar gum tended to be sufficiently viscous for successful paste extrusion and deposition as well as retaining their shape when dry [21, 22, 39]. Addition of calcium chloride as crosslinker [40, 41] resulted initially in greater viscosity and, as the calcium ion concentration rose, a decreased viscosity due to precipitation of protein and lignin. Greater starting keratin alkalinity required higher calcium chloride content to allow extrusion. Calcium chloride titrations of KLcar30 and KLgg30 solutions revealed highly alkaline compositions decreased in pH on calcium addition (Supplementary materials, Figure 1) with the final pH in the region expected for protein-polyphenol conjugation between keratin and lignin respectively [19], and for favoured hydrogel formation of keratin [21]. Collectively, this contributes understanding to the dependency of starting keratin-lignin hydrogel formulation pH and calcium chloride addition to achieve 3D print deposition of keratin-lignin composites.

Table 1. Survey of 3D paste printing characteristics of various keratin-lignin hydrogel formulations containing thickening agents and calcium chloride. Included are selected examples demonstrating optimal printing and dehydration characteristics

Formulation	Keratin-Lignin Composition (KL, (‡)) §,⁑	Composition (%)			% of additive relative to Keratin (%)	Calcium Chloride† (%)	Printable[Q] (Yes/ No/ Optimal)
		Keratin	Lignin	Additive			
-	K (pH 11, A)	100				<30	N
-	K (pH 12, B)	100				<25	N
1	KL (pH 9)	83	17	0		-	N
1A	KL (pH 10)	83	17	0		>5.5	N
1B	KL (pH 11)	83	17	0		5	N
2	KLcar8	78	16	6	8	>5.5	Y
2B	KLcar8	78	16	6	8	30	N
10	KLcar8	78	16	6	8	5	Y
3	KLcar(5	74	15	11	15	>2	Y
3B	KLcar15	74	15	11	15	>3	Y
11	KLcar15	74	15	11	15	3	Y
4	KLcar23	70	14	16	23	>2	Y
4B	KLcar23	70	14	16	23	>2	Y
12	KLcar23	70	14	16	23	2	Y
5	KLcar30	67	13	20	30	>2	Y
13	KLcar30	67	13	20	30	2.0	O
14A	KLcar30	67	13	20	30	4.5	O
5B	KLcar30	67	13	20	30	>5.5	Y
15B	KLcar30	67	13	20	30	7.5	O

6	KLgg8	78	16	6	8	5.5	Y
6B	KLgg8	78	16	6	8	5-6	Y
7	KLgg15	74	15	11	15	3.3	Y
17	KLgg15	74	15	11	15	3.5	O
7B	KLgg15	74	15	11	15	2-3	Y
8	KLgg23	70	14	16	23	2	Y
8B	KLgg23	70	14	16	23	>3	Y
18	KLgg23	70	14	16	23	2	Y
16	KLgg30	67	13	20	30	11	Y
9	KLgg30	67	13	20	30	2-4	Y
19	KLgg30	67	13	20	30	4.5	O
9A	KLgg30	67	13	20	30	4-5	Y
9B	KLgg30	67	13	20	30	2-5	Y
20	KLgg30	67	13	20	30	7.5	Y
21	KLgg30	67	13	20	30	19	Y

Where:

§ = KL combined keratin-lignin solution uses keratin solution at pH 8.3, pH 11 (A) or pH 12 (B).

‡ = % carrageenan (car) or guar gum (gg) addition on keratin (w/w) compared to the overall % composition of each component.

† = % calcium chloride addition on keratin (w/w)

O = examples of keratin-lignin hydrogel formulations exhibiting optimal 3D paste printing, formation and dehydration characteristics

3.2 *Characterisation of 3D printed hydrogel bars*

Shown in Figure 1 are scanning electron microscopy images of selected printed keratin-lignin hydrogel bars. Generally, despite their relatively smooth exteriors, the samples exhibit a relatively porous morphology typical of regenerated keratin materials [21, 39]. For carrageenan samples, the extent of this porosity appeared reduced at higher carrageenan loading. Similarly, for guar gum samples the porosity appeared lower at higher guar gum content with samples additionally associated with relatively smooth surfaces to these pores. However, for both carrageenan and guar gum samples **5** and **9**, the addition of calcium chloride led to increases in porosity and a reduction in the size of the pores. This was most apparent at >5% calcium content **(15**, **16**, **19**, **20**, see Table 2). Moreover, this porosity appeared more torturous with a jagged nature to the pore shape at higher calcium contents. It is evident this sample morphology resulted from a combination of protein cross-linking induced by calcium ions [39] combined with the shrinkage of the sample as the hydrogel dehydrated.

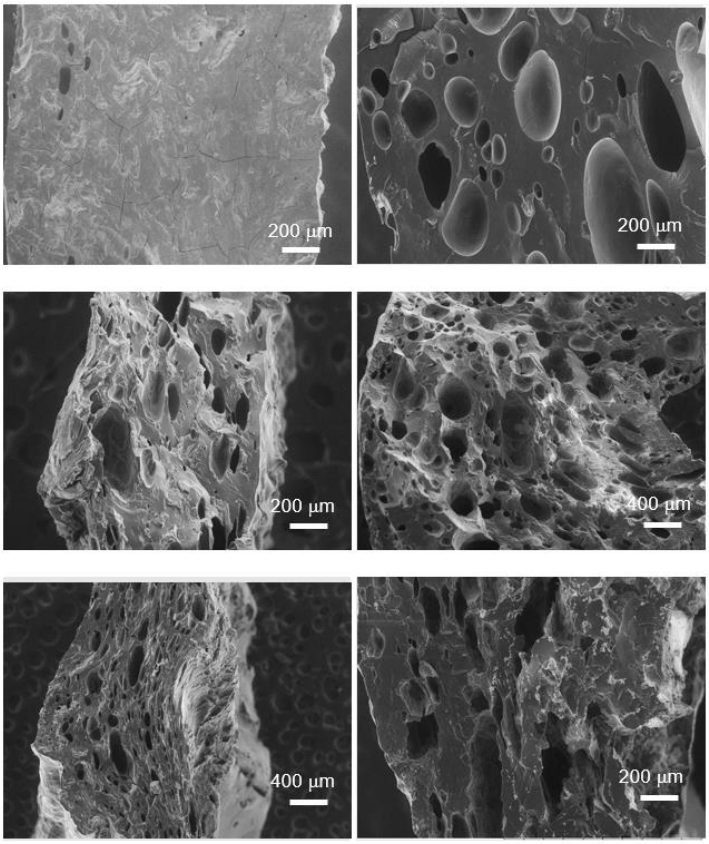

Figure 1. Representative scanning electron microscopy images of selected dried 3D printed keratin-lignin hydrogel bars containing either 30% carrageenan (left) or 30% guar gum (right) on keratin. Samples vary in calcium chloride content with 2.0% (top, **5**), 4.5% (middle, **14**), and 7.5% (bottom, **15**)

Shown in Figure 2 are differential scanning calorimetry (DSC) thermograms of selected printed hydrogel samples. Additives had a notable impact on the retention of absorbed water of equilibrated hydrogel samples. For KLcar30 (**5**) the first heating cycle thermogram showed an initial endotherm at *ca.* 70 °C for the loss of adsorbed water and a greater endotherm above 100 °C (125 °C maximum) attributable to bound water loss and polymer properties of the carrageenan and keratin components [42, 43]. In contrast, the second heating cycle of all samples was featureless, confirming that the initial endotherm was water loss. Addition of calcium chloride lessened the absorbed water contents of samples as evidenced by a common, broadened water loss endotherm for samples containing calcium (e.g. **14**). This effect of reduced moisture sorption was evident for KLcar30 samples with lower calcium chloride additions (**13**), with the extent of this water loss comparable to samples with lower carrageenan contents, particularly samples **2** and **3**. Addition of guar gum did not differentiate sample moisture losses below 100 °C with a broad endotherm evident below this temperature for all samples which was similar to analogous guar gum-containing KL samples produced by extrusion compounding at temperature [19]. However, the size of this water loss endotherm appeared proportionate to the guar gum content of compositions with a greater endotherm evident for KLgg23 (**8**) and KLgg30 (**9**) compared to KLgg8 (**6**).

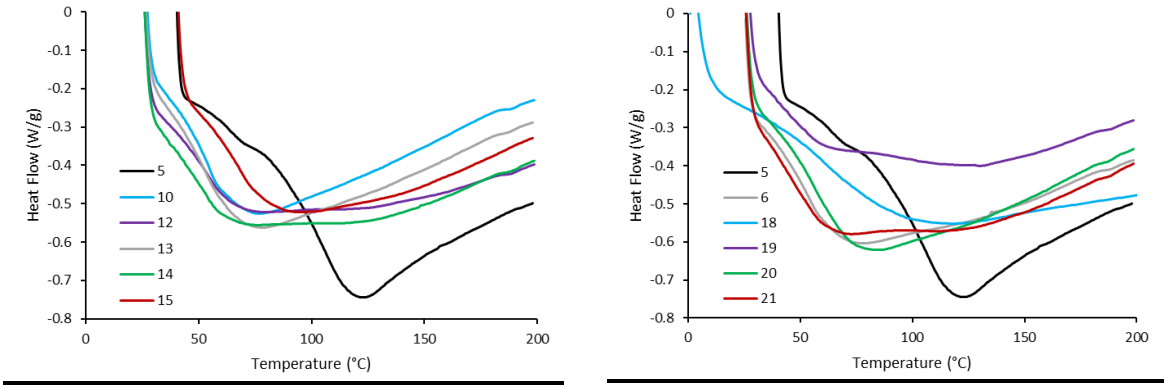

Figure 2. Differential scanning calorimeter thermograms for selected keratin-lignin hydrogels varying in carrageenan (left), guar gum (right) and calcium chloride contents. Legend numbers refer to numbers in Tables 1 and 2 and only the first heating cycle is shown

3.3 *Mechanical performance of 3D printed keratin-lignin materials*

Flexural testing of keratin-lignin printed bars varying in carrageenan, guar gum and calcium chloride contents was undertaken to assess the mechanical performance of these materials in their 3D printed hydrogel forms (Table 2. A combination of carrageenan and calcium chloride additions at lower contents led to an initial, stiffer KLcar material (**10**) with higher flexural strength. With higher carrageenan contents there was lower sample stiffness with MoE values observed to decrease to 1200 MPa (**13**) for those samples with 2-3% calcium chloride contents. The KLcar30 samples **14**–**16** with >4% calcium chloride loading demonstrated significant decreases in mechanical properties (200-300 MPa and <20 MPa for flexural modulus and strength, respectively). A greater carrageenan content had the effect of reducing %strain at break, consistent with the flexural properties of the KLcar30 materials noted above. The high calcium chloride contents (>4%) led to lower yield stress and a greater plasticization of the KLcar30 materials promoting their elongation at break.

For samples containing guar gum, mechanical testing indicated these materials were not impacted by the amount of this additive at lower calcium chloride contents (<3%, Table 2). Flexural modulus values tended to be *ca*. 700 MPa across KLgg samples **17** to **19**. Stress-strain behaviours were comparable across all KLgg samples, being distinguished only by their break loads. Nonetheless, as found with KLcar samples, higher calcium chloride contents (>5%) in KLgg samples led to greater plasticization behaviours and associated decreases in sample yield stress and flexural performance. Overall, it was evident higher calcium chloride contents decreased the flexural properties of keratin-lignin hydrogels, perhaps due to the agglomeration and precipitation of the protein, particularly with calcium additions above 4% (w/w keratin).

Table 2. Summary of flexural testing of selected hydrogel formulations as 3D printed bars

Sample	Keratin-Lignin Hydrogel Formulation	Modulus of Elasticity (MPa)		Flexural Strength (MPa)	
		Average	Standard Deviation	Average	Standard Deviation
5	KLcar30†	705	-	32	-
10	KLcar8 + 5% $CaCl_2$	1589	121	42	3
11	KLcar15 + 3% $CaCl_2$	1413	55	46	4
12	KLcar23 + 2% $CaCl_2$	1004	206	32	1
13	KLcar30 + 2% $CaCl_2$	1173	201	35	7
14	KLcar30 + 4.5% $CaCl_2$ †	257	-	14	-
15	KLcar30 + 7.5% $CaCl_2$ †	271	-	10	-
16	KLgg30 + 11% $CaCl_2$ †	195	-	5	-
6	KLgg30	912	262	33	0
17	KLgg15 + 3.5% $CaCl_2$	723	342	21	5
18	KLgg23 + 2% $CaCl_2$	602	232	13	4
19	KLgg30 + 4.5% $CaCl_2$	1019	667	35	14
20	KLgg30 + 7.5% $CaCl_2$ †	218	-	8	-
21	KLgg30 + 19% $CaCl_2$	390	97	8	1

† - Only one print specimen produced with sufficient quality for mechanical performance evaluations

3.4 *Keratin-lignin hydrogel moisture sorption responses*

Printed keratin-lignin hydrogel bars were exposed to differing humidity environments to understand impacts of their composition on water vapour transmission. Figure 3 shows the dynamic moisture responses of samples with humidity. Generally, conditioned samples (equilibrated at 65% RH, 20 °C) tended to lose moisture in drier humidity (40-60%) with sorption (weight gain) evident at higher humidity (≥80%, Figure 3). Samples containing carrageenan were found to be more responsive with greater rates of change than guar gum samples, irrespective of carrageenan content. Interestingly, for the KLcar30 samples the presence of calcium chloride in **13** contributed to a greater loss of moisture at 40% RH than for **5** (5.9 and 3.7%, respectively) suggesting an absence of the calcium additive contributes to greater hygroscopic retention of water within KLcar samples. At higher humidity, all KLcar samples show similar weight gains (0.8-1.2%) which was independent of their additive composition. In

contrast, guar gum containing samples did not exhibit significant %weight change across the differing humidity's (Figure 3). When alkalinity is considered, it was observed that pH had little effect on guar gum containing samples, but high pH carrageenan samples were more responsive to moisture. This distinction in moisture sorption is also consistent with the properties of guar gum and carrageenan where the latter has a high response to moisture changes with temperature and humidity[37] compared to guar gum[38].

Overall, vapour transmission testing has indicated the carrageenan-containing KLcar samples have a greater response to changes in ambient humidity and employing a higher alkaline pH enhanced this responsiveness of hydrogel formulations.

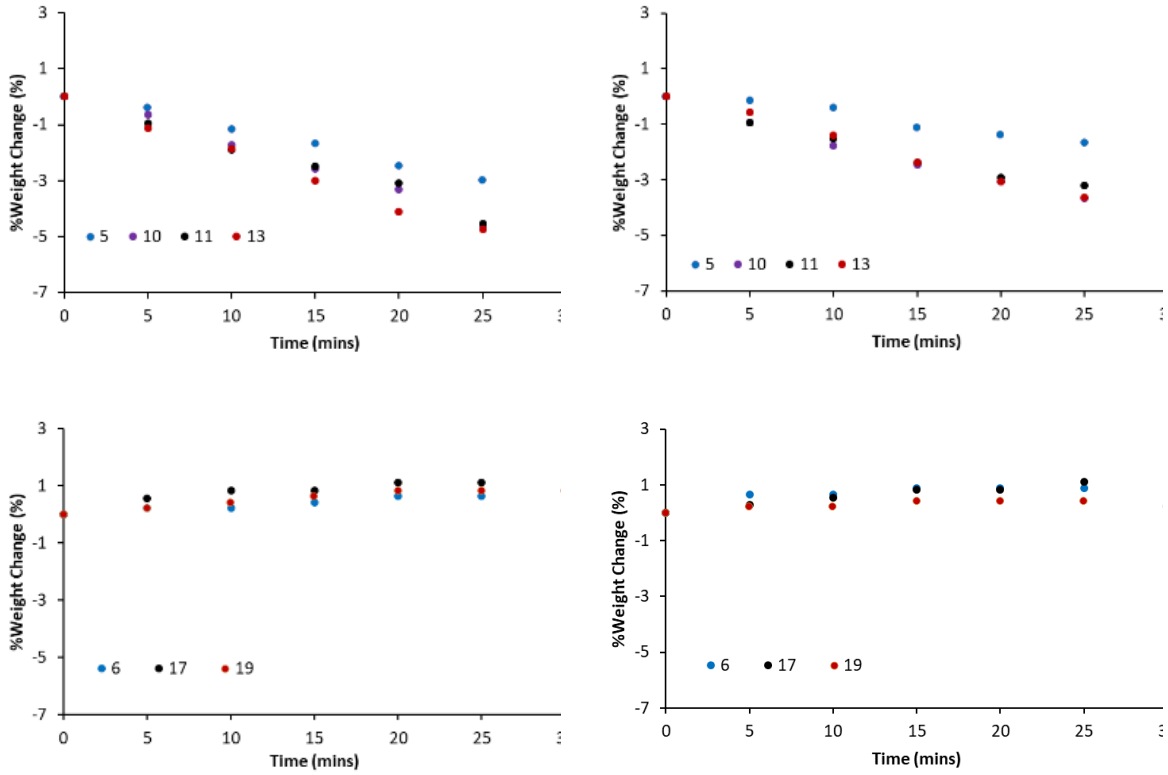

Figure 3. Dynamic water vapour sorption profiles of selected 3D printed hydrogel bars at 40% (left) and 60% (right) relative humidity's (at 20 °C). Carrageenan-containing KLcar samples (top) and guar gum-containing KLgg samples (bottom). Legend numbers refer to sample numbers in Tables 1 and 2

Having established influences of KL hydrogel formulation composition on water vapour transmission rates, printed bar samples were subjected to liquid water immersion. All samples absorbed water over the testing timeframe (30 mins, Figure 4), consistent with previous water immersion experiments [19]. The rates of water absorptivity were variable across samples reflecting both compositional differences and, arguably, sample integrity. Samples with increasing carrageenan content had very differing water sorption rates, exemplified by KLcar8 (**2**) and KLcar30 (**5**) having water sorption uptakes of >1000% and 230% (w/w), respectively. Other carrageenan-containing samples generally had uptakes of 200-300% (w/w) over 30 mins. The inclusion of calcium chloride modified these liquid water uptakes. On water immersion the KLcar8 (10), KLcar15 (**11**) and KLcar30 (**13**) samples with low calcium contents all have comparable water sorption profiles and uptake (ca. 270%). For KLcar30 samples an increasing calcium chloride content generally had the effect of reducing water absorption. Water sorption was reduced to *ca*. 160% with 11% calcium chloride (**16**) with lower additions proving to have a variable effect which was likely attributable to the print deposition and integrity of these printed hydrogels (Figure 1).

Keratin-lignin samples containing guar gum (KLgg) were distinguished by comparatively greater uptakes on water immersion (Figure 4). For this series, weight uptakes ranged between 200 and 500% across samples with less than 7% calcium chloride and were not distinguished by their guar gum contents. For the KLgg30 sample series, progressive increases of calcium chloride had the effect of reducing the rate of water uptake, with 10-20%

calcium chloride content reducing the %weight uptake to *ca.* 200% (**21**). In contrast, calcium chloride contents less than 5% provided little benefit of reducing water uptake and corroborate observations with KLcar samples.

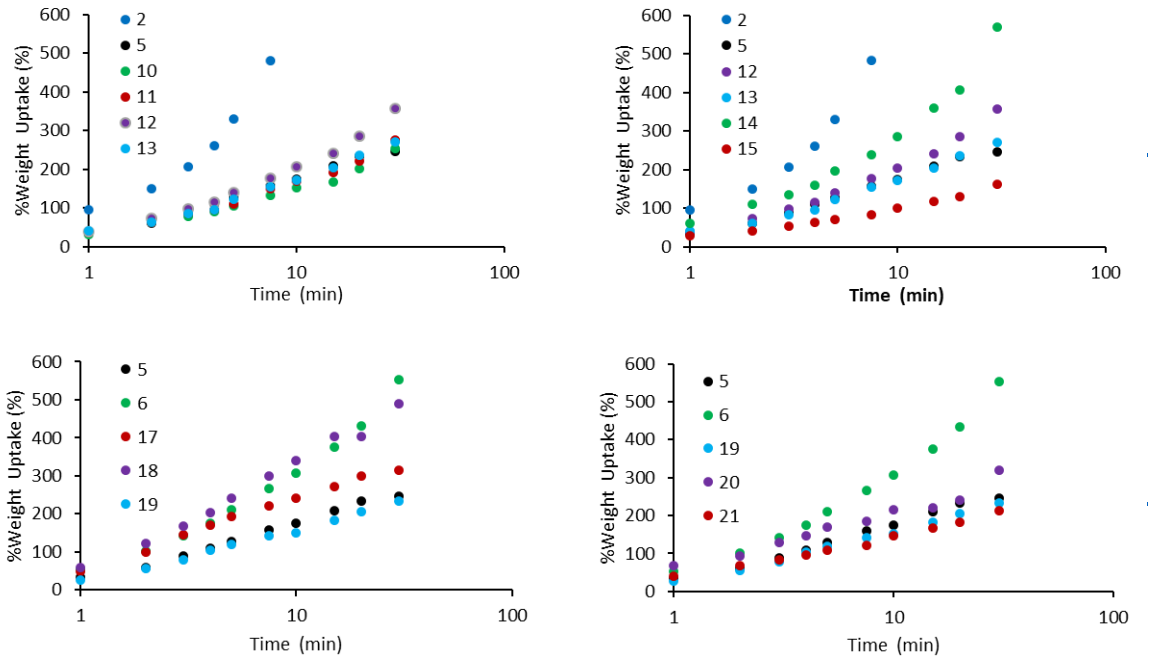

Figure 4. Comparisons of water uptake on water immersion for selected 3D printed keratin-lignin hydrogel formulations containing carrageenan, guar gum and calcium chloride modifiers. Carrageenan-containing KLcar samples (top) and guar gum-containing KLgg samples (bottom) with time axis in log scale. Legend numbers refer to sample numbers in Tables 1 and 2

To further develop keratin-lignin material responses to liquid water, selected samples were acidified to benefit from advantageous properties exhibited by keratin hydrogels at the protein isoelectric point [44]. Both KLcar and KLgg printed bars were modified by dilute acetic acid immersion with time-based treatment levels of 10 to 300 seconds, timings in which only low liquid uptakes were observed (Figure 4). The resulting acidification of printed bars was found to have a significant impact on sample water uptakes (Figure 5). This was exemplified by acid-treated KLcar30 samples which demonstrated water uptakes ranging from 100 to >500% compared to the untreated KLcar30 sample (**5**, 240%). For KLcar30 samples containing 2-5% calcium chloride, samples showed significantly reduced water uptakes upon acid post-treatment including **14** which had a water uptake of only *ca.* 100%. This low water uptake value was maximised after 120 seconds acid treatment immersion with shorter times also proving beneficial (<200%) compared with 300% uptake for untreated **14**. At a lower calcium chloride level (2%, **13**) acid treatment was also slightly beneficial to reducing water sorption, with results between those of acid treated samples **5** and **14**. Interestingly, for samples containing guar gum, the effects of printed bar acid treatment were capricious as found for **19** (4.5% $CaCl_2$, Figure 5). It is likely this variable response to acidification and water uptake reflect the poorer water resistance exhibited by untreated guar gum samples on water immersion (Figure 4).

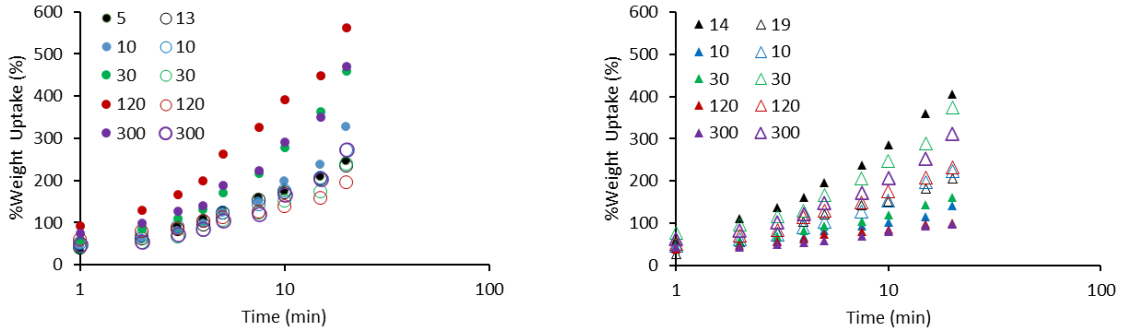

Figure 5. Comparisons water uptakes on water immersion of selected 3D printed keratin-lignin hydrogel formulations having undergone acidification via acetic acid treatment. Samples **5** and **13** (left) and samples **14** and **19** (right). Untreated samples (black) with acidification times of 10 (blue), 30 (green), 120 (red) and 300 (purple) seconds. Legend numbers refer to numbers in Tables 1 and 2

3.5 *Mechanical performance of keratin-lignin hydrogel materials on water immersion*

Assessments of 3D printed hydrogel mechanical properties on their water immersion were undertaken to evaluate the impacts of keratin-lignin additives on material performance (Figure 6,). Generally, all samples were observed to soften on immersion with this being similar to moisture-induced plasticization previously observed for keratin-lignin materials compressed in dry-form [19]. Across the KLcar series there were distinctions in the rate of sample softening and plasticization contributed by both carrageenan and calcium chloride additions. At low carrageenan content, both KLcar8 (**2**) and KLcar23 (**4**) show a greater initial stiffness loss consistent with their water absorption behaviours (Figure 4). Furthermore, with extended water immersion each was observed to achieve maximum moisture-induced softening within 60 mins, before deteriorating with excessive swelling. For KLCar30 (**5**), the lower water uptake rate exhibited by this sample was also conveyed in the initial softening behaviour however, this sample too, fully softened within 60 mins of immersion. Those KLcar30 samples differing in calcium chloride content were found to vary in their rates of softening. At lower calcium chloride additions (**13**, **14**), samples show a slower initial stiffness loss on water immersion which was consistent with their respective water uptakes (Figure 8) and mechanical properties (Table 2). The performance of these samples extended beyond 150 mins (Supplementary Materials). In contrast, a higher calcium chloride content (**15**, 7.5%) had an adverse effect, revealing the capricious effects of additives on sample plasticization and moisture responsiveness. For **15**, a 7.5% calcium chloride content contributed to greater initial softening consistent with the greater plasticization of this material observed in stress strain behaviours (Figure 4). However, this sample demonstrated extended performance in water (>230 min) which can be attributed to greater water resistance and sample integrity provided by protein crosslinking [40, 41]. The extended performance of **15** on water immersion was comparable to keratin-lignin materials produced in dry-form [19]. Lastly, the low water resistance shown by guar gum samples was also reflected in mechanical properties on water immersion where, for example, the integrity of KLgg30 (**21**) was compromised within 30 mins. Overall, these water immersion evaluations (Figure 10) demonstrate the water responsiveness and behaviour on initial wetting of keratin-lignin hydrogel materials and how higher rates of water absorption will contribute to plasticization and softening and impact the mechanical performance of these materials.

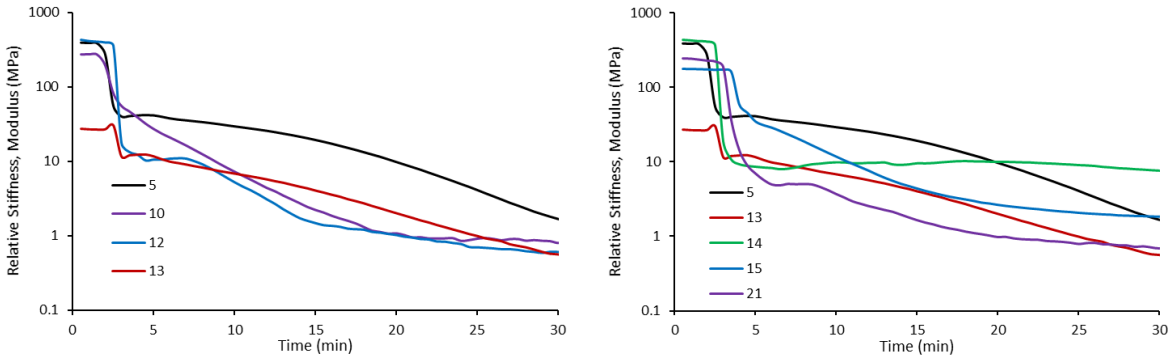

Figure 6. Dynamic mechanical analysis of selected 3D printed keratin-lignin hydrogel bars demonstrating material responses on water immersion at ambient temperature (23 °C). Samples tested in 3 point bending and vary in carrageenan content (left) and calcium chloride content and guar gum (right). See Supplementary Materials for sample performance at extended immersion times. Legend numbers refer to numbers in Tables 1 and 2

3.6 *Discussion*

Study outcomes have revealed the complexities of using additives to modify 3D printed keratin-lignin hydrogel deposition and their resulting 4D material performance and moisture responsiveness. As formulation thickeners, both carrageenan and guar gum modified hydrogel formulations improving the 3D printing deposition quality and material characteristics. However, only carrageenan additionally contributed to enhanced mechanical properties and the 4D moisture sorption behaviours of the printed hydrogel materials. While the trends in printability for both carrageenan and guar gum additions were likely a balance of the %solids, composition and keratin content in hydrogel formulations (Table 1), alongside the additive content, printability results indicate a

pH effect to printability as the alkalinity of keratin and lignin solutions also impacted deposition and dehydration of 3D printed bars (Table 1).

Of those preferred keratin-lignin hydrogel formulations exhibiting favourable 3D print deposition characteristics (Table 1), these were not representative of the most desired mechanical and moisture sorption properties. A lower carrageenan content contributed greater mechanical performance of printed hydrogel materials than use of carrageenan at >20% contents, with this reinforcement further reduced at high calcium chloride loadings (Table 2). However, employing a greater carrageenan content was associated with higher water vapour sorption responsiveness (Figure 5). Carrageenan-modified samples were more dynamic in their rates of moisture sorption with the high content carrageenan KLcar30 samples (e.g. **5** and **13**) having the greatest rates of vapour transmission (0.1 - 0.2% wt/min) compared to guar gum samples (<0.05% wt/min, Figure 6). The impact of guar gum additions on keratin-lignin hydrogel performance was significantly lower, contributing only modest mechanical performance improvements in combination with calcium chloride (Table 2). This limiting effectiveness of guar gum modification was also conveyed in hydrogel moisture responsiveness with minimal impacts on vapour sorption behaviours (Figure 6) and water immersion (Figure 10) when compared to use of carrageenan, particularly at higher contents. These results suggest modified hydrogels include carrageenan to tune both sample mechanical properties and moisture responses, whereas guar gum use will provide a neutral effect, acting only to improve formulation print viscosity (Table 1).

While calcium chloride inclusion revealed the capricious nature of modified keratin-lignin hydrogels, there was a defined content which provided beneficial material properties. Firstly, an increasing calcium chloride addition and associated protein cross-linking [40, 41] had the effect of changing hydrogel morphology (Figure 2) with this also impacting mechanical performance at higher loadings (Table 2). At greater than 5% calcium chloride (**14**, **15**), this additive had the effect of plasticising the hydrogel and inducing differing stress-strain behaviours of calcium-modified hydrogel materials (Figure 4). However, any reinforcement provided by calcium chloride inclusion also acted to reduce ambient water vapour sorption as well as slow liquid water ingress into the hydrogel and significantly extend mechanical performance on water immersion (Figures 3, 5, 8 and 10). These responses, particularly on liquid water immersion, suggest calcium chloride should be used in combination with carrageenan in preference to guar gum and that a range of keratin-lignin hydrogel properties are possible on their selective combination. For example, in this study sample **15** was favoured for liquid water immersion, whereas **13** demonstrated both superior mechanical performance and water vapour responsiveness.

Post-acidification of deposited keratin-lignin hydrogel materials also conferred differing moisture responses with the calcium chloride content important for this attribute. There was a time dependency to the efficacy of sample acidification with shorter treatments proving better for reducing water uptakes compared to extended acidification treatment (Figure 9). For example, for acid treated **13** samples, a 30–120 sec immersion proved better than an extended treatment (300 sec). This efficacy was gained by acidification reducing both the keratin and lignin pH toward their respective isoelectric points to improve water resistance [44]. However, extended acidification treatment likely results in solubilisation of calcium ions giving a reduced cross-linked hydrogel network leading to greater water sorption and poorer performance as seen with samples prepared without calcium ions (**5**, Figures 8, 9 and 10). Interestingly, for samples containing guar gum, the effects of printed bar acid post-treatment were capricious as exemplified by **19** which had mixed liquid water uptakes after acidification. Guar gum, a galactomannan polysaccharide, does not readily combine with proteins without the presence of additional crosslinkers [45, 46] so any crosslinking of the hydrogel components provided by calcium will be lost with acid treatment. This is not the case with the anionic polysaccharide carrageenan which is known to cross-link proteins [47, 48] and provide the beneficial properties exhibited in mechanical testing (Table 2). It was evident from this evaluation, further work will be required to develop and optimise acidification post-treatments of the 3D printed hydrogel materials.

4. Summary

Overall, study findings direct the use of additives to tailor 3D print deposition of keratin-lignin hydrogels and their 4D material moisture responsiveness. Carrageenan proved a functional additive, contributing to material performance, particularly in combination with calcium chloride, whereas guar gum only contributed to improved printability of hydrogel formulations. Addition of carrageenan to hydrogel formulations led to improved material stiffness and greater water vapour sorption behaviours. This was further enhanced by calcium ions, particularly for hydrogel materials immersed in water. These 4D material responses were detrimentally impacted by higher calcium chloride contents, decreasing mechanical performance of keratin-lignin hydrogels, particularly calcium chloride additions above 4%. The demonstration of 4D characteristics and moisture-induced softening reveal the

potential of hydrogels and their use as hygromorphic materials responding to changing humidity or liquid water with a range of end-use applications possible. Desired performances of 3D printed keratin-lignin materials can be tailored through selection of composition and additive choice and, through smart design, how these hydrogels may be applied including emerging concepts of 2 layer 3D print depositions in combination with hydrophobic materials.

Acknowledgments

The authors are grateful to The Science for Technological Innovation National Science Challenge (SfTI) and the Strategic Science Investment Fund (AgResearch Limited and Scion) for funding of this research. H.W. was a recipient of an AgResearch summer studentship scholarship.

References

[1] D'aveni R. The 3-D Printing Revolution. Harvard Business Review. 2015.
[2] Altomare, L.; Bonetti, L.; E Campiglio, C.; De Nardo, L.; Draghi, L.; Tana, F.; Farè, S. Biopolymer-based strategies in the design of smart medical devices and artificial organs. *Int. J. Artif. Organs* **2018**, *41*, 337–359, https://doi.org/10.1177/0391398818765323.
[3] Kuang, X.; Roach, D.J.; Wu, J.; Hamel, C.M.; Ding, Z.; Wang, T.; Dunn, M.L.; Qi, H.J. Advances in 4D Printing: Materials and Applications. *Adv. Funct. Mater.* **2018**, *29*, https://doi.org/10.1002/adfm.201805290.
[4] Mitchell, A.; Lafont, U.; Hołyńska, M.; Semprimoschnig, C. Additive manufacturing — A review of 4D printing and future applications. *Addit. Manuf.* **2018**, *24*, 606–626, https://doi.org/10.1016/j.addma.2018.10.038.
[5] Ahmed A, Arya S, Gupta V, Furukawa H, Khosla A. 4D printing: Fundamentals, materials, applications and challenges. Polymer. 2021;228.
[6] Alshahrani, H.A. Review of 4D printing materials and reinforced composites: Behaviors, applications and challenges. *J. Sci. Adv. Mater. Devices* **2021**, *6*, 167–185, https://doi.org/10.1016/j.jsamd.2021.03.006.
[7] Biswas, M.C.; Chakraborty, S.; Bhattacharjee, A.; Mohammed, Z. 4D Printing of Shape Memory Materials for Textiles: Mechanism, Mathematical Modeling, and Challenges. *Adv. Funct. Mater.* **2021**, *31*, 2100257, https://doi.org/10.1002/adfm.202100257.
[8] Manshor, M.R.; Alli, Y.A.; Anuar, H.; Ejeromedoghene, O.; Omotola, E.O.; Suhr, J. 4D printing: Historical evolution, computational insights and emerging applications. *Mater. Sci. Eng. B* **2023**, *295*, https://doi.org/10.1016/j.mseb.2023.116567.
[9] Shinde, S.; Mane, R.; Vardikar, A.; Dhumal, A.; Rajput, A. 4D printing: From emergence to innovation over 3D printing. *Eur. Polym. J.* **2023**, *197*, https://doi.org/10.1016/j.eurpolymj.2023.112356.
[10] Correa, D.; Poppinga, S.; Mylo, M.D.; Westermeier, A.S.; Bruchmann, B.; Menges, A.; Speck, T. 4D pine scale: biomimetic 4D printed autonomous scale and flap structures capable of multi-phase movement. *Philos. Trans. R. Soc. A: Math. Phys. Eng. Sci.* **2020**, *378*, 20190445, https://doi.org/10.1098/rsta.2019.0445.
[11] Hess, K.M.; Killgore, J.P.; Srubar, W.V. Nanoscale hygromechanical behavior of lignin. *Cellulose* **2018**, *25*, 6345–6360, https://doi.org/10.1007/s10570-018-2045-3.
[12] Johnson, K.; Trim, M.; Francis, D.; Whittington, W.; Miller, J.; Bennett, C.; Horstemeyer, M. Moisture, anisotropy, stress state, and strain rate effects on bighorn sheep horn keratin mechanical properties. *Acta Biomater.* **2017**, *48*, 300–308, https://doi.org/10.1016/j.actbio.2016.10.033.
[13] Kretschmann D. Natural materials: Velcro mechanics in wood. Nature Materials. 2003;2(12):775-6.
[14] Popescu C. The thermodynamics of trichocyte keratins. Advances in Experimental Medicine and Biology: Springer New York LLC; 2018. p. 185-203.
[15] Choi, W.S.; Kim, J.H.; Ahn, C.B.; Lee, J.H.; Kim, Y.J.; Son, K.H.; Lee, J.W. Development of a Multi-Layer Skin Substitute Using Human Hair Keratinic Extract-Based Hybrid 3D Printing. *Polymers* **2021**, *13*, 2584, https://doi.org/10.3390/polym13162584.
[16] Ghosh, S.; Chaudhuri, S.; Roy, P.; Lahiri, D. 4D Printing in Biomedical Engineering: a State-of-the-Art Review of Technologies, Biomaterials, and Application. *Regen. Eng. Transl. Med.* **2023**, *9*, 339–365, https://doi.org/10.1007/s40883-022-00288-5.
[17] Martella, E.; Ferroni, C.; Guerrini, A.; Ballestri, M.; Columbaro, M.; Santi, S.; Sotgiu, G.; Serra, M.; Donati, D.M.; Lucarelli, E.; et al. Functionalized Keratin as Nanotechnology-Based Drug Delivery System for the Pharmacological Treatment of Osteosarcoma. *Int. J. Mol. Sci.* **2018**, *19*, 3670, https://doi.org/10.3390/ijms19113670.

[18] Flores-Hernandez CG, Murillo-Segovia B, Martinez-Hernandez AL, C V-S. Keratin as Renewable Material to Develop Polymer Composites: Natural and Synthetic Matrices. Handbook of Composites from Renewable Materials. p. 1-29.
[19] Grigsby, W.J.; Scott, S.M.; Plowman-Holmes, M.I.; Middlewood, P.G.; Recabar, K. Combination and processing keratin with lignin as biocomposite materials for additive manufacturing technology. *Acta Biomater.* **2020**, *104*, 95–103, https://doi.org/10.1016/j.actbio.2019.12.026.
[20] Liu, J.; Sun, L.; Xu, W.; Wang, Q.; Yu, S.; Sun, J. Current advances and future perspectives of 3D printing natural-derived biopolymers. *Carbohydr. Polym.* **2019**, *207*, 297–316. https://doi.org/10.1016/j.carbpol.2018.11.077.
[21] Hedegaard CL, Collin EC, Redondo-Gómez C, Nguyen LTH, Ng KW, Castrejón-Pita AA, et al. Hydrodynamically Guided Hierarchical Self-Assembly of Peptide–Protein Bioinks. Advanced Functional Materials. 2018;28(16).
[22] Placone, J.K.; Navarro, J.; Laslo, G.W.; Lerman, M.J.; Gabard, A.R.; Herendeen, G.J.; Falco, E.E.; Tomblyn, S.; Burnett, L.; Fisher, J.P. Development and Characterization of a 3D Printed, Keratin-Based Hydrogel. *Ann. Biomed. Eng.* **2016**, *45*, 237–248, https://doi.org/10.1007/s10439-016-1621-7.
[23] Nguyen, N.A.; Barnes, S.H.; Bowland, C.C.; Meek, K.M.; Littrell, K.C.; Keum, J.K.; Naskar, A.K. A path for lignin valorization via additive manufacturing of high-performance sustainable composites with enhanced 3D printability. *Sci. Adv.* **2018**, *4*, eaat4967, https://doi.org/10.1126/sciadv.aat4967.
[24] Xu, W.; Wang, X.; Sandler, N.; Willför, S.; Xu, C. Three-Dimensional Printing of Wood-Derived Biopolymers: A Review Focused on Biomedical Applications. *ACS Sustain. Chem. Eng.* **2018**, *6*, 5663–5680, https://doi.org/10.1021/acssuschemeng.7b03924.
[25] Lai, H.Y.; Setyawati, M.I.; Ferhan, A.R.; Divakarla, S.K.; Chua, H.M.; Cho, N.-J.; Chrzanowski, W.; Ng, K.W. Self-Assembly of Solubilized Human Hair Keratins. *ACS Biomater. Sci. Eng.* **2020**, *7*, 83–89, https://doi.org/10.1021/acsbiomaterials.0c01507.
[26] Cera, L.; Gonzalez, G.M.; Liu, Q.; Choi, S.; Chantre, C.O.; Lee, J.; Gabardi, R.; Choi, M.C.; Shin, K.; Parker, K.K. A bioinspired and hierarchically structured shape-memory material. *Nat. Mater.* **2020**, *20*, 242–249, https://doi.org/10.1038/s41563-020-0789-2.
[27] Ajdary, R.; Kretzschmar, N.; Baniasadi, H.; Trifol, J.; Seppälä, J.V.; Partanen, J.; Rojas, O.J. Selective Laser Sintering of Lignin-Based Composites. *ACS Sustain. Chem. Eng.* **2021**, *9*, 2727–2735, https://doi.org/10.1021/acssuschemeng.0c07996.
[28] Ebers, L.; Arya, A.; Bowland, C.C.; Glasser, W.G.; Chmely, S.C.; Naskar, A.K.; Laborie, M. 3D printing of lignin: Challenges, opportunities and roads onward. *Biopolym.* **2021**, *112*, e23431, https://doi.org/10.1002/bip.23431.
[29] Gregor-Svetec, D.; Leskovšek, M.; Leskovar, B.; Elesini, U.S.; Vrabič-Brodnjak, U. Analysis of PLA Composite Filaments Reinforced with Lignin and Polymerised-Lignin-Treated NFC. *Polymers* **2021**, *13*, 2174, https://doi.org/10.3390/polym13132174.
[30] Hong, S.-H.; Park, J.H.; Kim, O.Y.; Hwang, S.-H. Preparation of Chemically Modified Lignin-Reinforced PLA Biocomposites and Their 3D Printing Performance. *Polymers* **2021**, *13*, 667, https://doi.org/10.3390/polym13040667.
[31] Chang, S.; Weng, Z.; Zhang, C.; Jiang, S.; Duan, G. Cellulose-Based Intelligent Responsive Materials: A Review. *Polymers* **2023**, *15*, 3905, https://doi.org/10.3390/polym15193905.
[32] Ahmed EM. Hydrogel: Preparation, characterization, and applications: A review. Journal of Advanced Research. 2015;6(2):105-21.
[33] Athamneh, A.I.; Griffin, M.; Whaley, M.; Barone, J.R. Conformational Changes and Molecular Mobility in Plasticized Proteins. *Biomacromolecules* **2008**, *9*, 3181–3187, https://doi.org/10.1021/bm800759g.
[34] Mendis, G.P.; Hua, I.; Youngblood, J.P.; Howarter, J.A. Enhanced dispersion of lignin in epoxy composites through hydration and mannich functionalization. *J. Appl. Polym. Sci.* **2014**, *132*, https://doi.org/10.1002/app.41263.
[35] Mimini, V.; Sykacek, E.; Hashim, S.N.A.S.; Holzweber, J.; Hettegger, H.; Fackler, K.; Potthast, A.; Mundigler, N.; Rosenau, T. Compatibility of Kraft Lignin, Organosolv Lignin and Lignosulfonate With PLA in 3D Printing. *J. Wood Chem. Technol.* **2019**, *39*, 14–30, https://doi.org/10.1080/02773813.2018.1488875.
[36] Johnson NAG, Russell IM. Advances in Wool Technology: Elsevier Ltd; 2008. 1-342 p.
[37] Torres, M.D.; Chenlo, F.; Moreira, R. Structural features and water sorption isotherms of carrageenans: A prediction model for hybrid carrageenans. *Carbohydr. Polym.* **2018**, *180*, 72–80, https://doi.org/10.1016/j.carbpol.2017.10.010.
[38] Torres, M.D.; Moreira, R.; Chenlo, F.; Vázquez, M.J. Water adsorption isotherms of carboxymethyl cellulose, guar, locust bean, tragacanth and xanthan gums. *Carbohydr. Polym.* **2012**, *89*, 592–598, https://doi.org/10.1016/j.carbpol.2012.03.055.
[39] Vu, T.; Xue, Y.; Vuong, T.; Erbe, M.; Bennet, C.; Palazzo, B.; Popielski, L.; Rodriguez, N.; Hu, X. Comparative Study of Ultrasonication-Induced and Naturally Self-Assembled Silk Fibroin-Wool Keratin Hydrogel Biomaterials. *Int. J. Mol. Sci.* **2016**, *17*, 1497, https://doi.org/10.3390/ijms17091497.

[40] Mukherjee, A.; Kabutare, Y.H.; Ghosh, P. Dual crosslinked keratin-alginate fibers formed via ionic complexation of amide networks with improved toughness for assembling into braids. *Polym. Test.* **2019**, *81*, 106286, https://doi.org/10.1016/j.polymertesting.2019.106286.
[41] Yan, J.; Liang, X.; Ma, C.; McClements, D.J.; Liu, X.; Liu, F. Design and characterization of double-cross-linked emulsion gels using mixed biopolymers: Zein and sodium alginate. *Food Hydrocoll.* **2020**, *113*, 106473, https://doi.org/10.1016/j.foodhyd.2020.106473.
[42] Ullah, A.; Vasanthan, T.; Bressler, D.; Elias, A.L.; Wu, J. Bioplastics from Feather Quill. *Biomacromolecules* **2011**, *12*, 3826–3832, https://doi.org/10.1021/bm201112n.
[43] Chaisawang, M.; Suphantharika, M. Effects of guar gum and xanthan gum additions on physical and rheological properties of cationic tapioca starch. *Carbohydr. Polym.* **2005**, *61*, 288–295, https://doi.org/10.1016/j.carbpol.2005.04.002.
[44] Ren Y, Yu X, Li Z, Liu D, Xue X. Fabrication of pH-responsive TA-keratin bio-composited hydrogels encapsulated with photoluminescent GO quantum dots for improved bacterial inhibition and healing efficacy in wound care management: In vivo wound evaluations. Journal of Photochemistry and Photobiology B: Biology. 2020;202.
[45] Das, A.; Das, A.; Basu, A.; Datta, P.; Gupta, M.; Mukherjee, A. Newer guar gum ester/chicken feather keratin interact films for tissue engineering. *Int. J. Biol. Macromol.* **2021**, *180*, 339–354, https://doi.org/10.1016/j.ijbiomac.2021.03.034.
[46] Sorde, K.L.; Ananthanarayan, L. Effect of transglutaminase treatment on properties of coconut protein-guar gum composite film. *LWT* **2019**, *115*, https://doi.org/10.1016/j.lwt.2019.108422.
[47] Ge, A.; Iqbal, S.; Chen, X.D. Alteration in rheology and microstructure of O/W emulsions using controlled soy protein isolate-polysaccharide aggregation in aqueous phases. *J. Food Eng.* **2022**, *317*, https://doi.org/10.1016/j.jfoodeng.2021.110872.
[48] Yan, J.-N.; Xue, S.; Du, Y.-N.; Wang, Y.-Q.; Xu, S.-Q.; Wu, H.-T. Influence of pH and blend ratios on the complex coacervation and synergistic enhancement in composite hydrogels from scallop (patinopecten yessoensis) protein hydrolysates and κ-carrageenan/xanthan gum. *LWT* **2021**, *154*, 112745, https://doi.org/10.1016/j.lwt.2021.112745.